Publications of the Astronomical Society of the Pacific
107: 945–958, 1995 October

Galaxy Colors in Various Photometric Band Systems

M. FUKUGITA[1]

Institute for Advanced Study, Princeton, New Jersey 08540
Electronic mail: fukugita@sns.ias.edu

K. SHIMASAKU[2]

Princeton University Observatory, Princeton, New Jersey 08544
Electronic mail: shima@astro.princeton.edu

T. ICHIKAWA

Kiso Observatory, University of Tokyo, Kiso-gun, Nagano 397-01, Japan
Electronic mail: ichikawa@kikyo.kiso.ioa.s.u-tokyo.ac.jp

Received 1995 March 10; accepted 1995 June 14

ABSTRACT. A study is made of stellar and galaxy colors using a spectrophotometric synthesis technique. We show that use of good color response functions and a modern determination of the spectroscopic energy distribution for α Lyr gives synthetic stellar colors in a good agreement with photometric observations to about 0.05 mag. The synthetic method then is applied to study galaxy colors using the spectrophotometric atlas of Kennicutt (1992, ApJS, 79, 255), and a comparison is made with observed galaxy colors. The K correction is calculated and compared with that of Coleman, Wu, and Weedman (1980, ApJS, 43, 393). We then study colors of galaxies in various photometric band systems and obtain color transformation laws, which enable us to find offsets among different systems. We include 48 photometric bands in our study.

1. INTRODUCTION

Colors of galaxies provide us with valuable information concerning their present-day composition of stars, and accordingly it gives us hints about the formation and evolution of galaxies. While a large number of studies have been made in this area, different authors have usually used varieties of different photometric band systems. Indeed, each photometric band system has its own advantages. This causes, however, great complications for the analysis of the accumulated data in a coherent way. To solve this problem, the author usually gives a transformation law from his own photometric system to another, which is more frequently adopted, in terms of empirical color–color relations. If we want to transform one magnitude to another, which is not given directly by the author, however, we must combine empirical relations successively for a number of times, which often leads to inaccurate results; we occasionally find that the results depend on how these relations are combined. Furthermore, the laws given by different authors sometimes disagree, and it is difficult to trace the origin of discrepancies, since these laws are derived using different standard stars.

An alternative way to give transformation laws among different colors is to synthetically calculate magnitude using the spectroscopic energy distribution (SED) of galaxies and the filter response functions. Such attempts, however, are not popular. The reason is that it requires accurate response functions, and also an accurate continuous SED of α Lyr (Vega), used to define a zero point of the standard magnitude system, in addition to a good sample of galaxy SED over a wide range of wavelength. Continual efforts to obtain the SED of Vega (Oke and Schild 1970; Hayes and Latham 1975; Oke and Gunn 1983; Kurucz 1979; Hayes 1985, hereafter referred to as H85; Castelli and Kurucz 1994, hereafter referred to as CK94) and response functions (e.g., Code 1960; Arp 1961; Matthews and Sandage 1963; Azusienis and Straizys 1969; Hayes 1975; Buser 1978; Bessell 1990), however, lead us to expect that the error from the first two issues can now be controlled to a tolerable level for our purpose. We also have a reasonable amount of spectrophotometric data for a few dozens of galaxies. This prompts us to carry out a synthetic study of galaxy colors in various band systems and to obtain transformation laws among them. With this calculation we can directly estimate the offset between two different magnitude systems, which is important in, for example, number counts of galaxies.

In this paper we carry out a synthetic study of galaxy colors using the best modern data available. In order to see the general accuracy of the method, we first compute broad band stellar colors using the SED of stars (Jacoby, Hunter and Christian 1984; Gunn and Stryker 1982) and compare them with observed colors (Sec. 1). Such studies have been made from time to time by many authors. The new feature of our calculation is that we use directly the SED of α Lyr to set the zero point, rather than resorting to an empirical relation. We then calculate broadband colors from SED of galaxies, comparing them with observations, and briefly discuss the color distribution of galaxies (Sec. 3). With these preparations, we calculate colors of galaxies in various photometric band systems for galaxies at $z=0$ and higher redshifts. We then compute color transformation laws among various photometric band systems (Sec. 4).

[1]Also at Yukawa Institute, Kyoto University, Kyoto 606 Japan.
[2]On leave from Department of Astronomy, University of Tokyo, Tokyo 113, Japan.

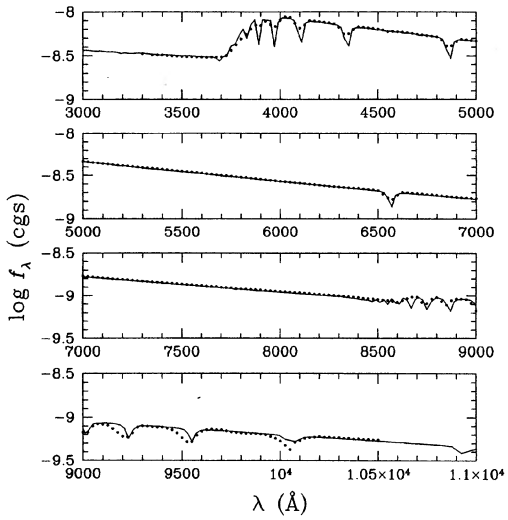

FIG. 1—Comparison of the H85 SED of α Lyr (dots) with that of CK94 (solid curve). The wavelength scale is enlarged to emphasize the small discrepancy between the two.

After completion of this work we find parallel work by Frei and Gunn (1994), who computed colors and K corrections of galaxies for five photometric systems, using an SED of Coleman, Wu, and Weedman (1980) with the zero point of photometric systems calibrated with the SED of F subdwarfs. Our present study is a substantially more systematic exploration of the subject with a number of checks needed to define accurate photometric systems.

2. SYNTHETIC STELLAR COLORS FOR THE STANDARD JOHNSON/COUSINS SYSTEM

A number of studies have been done for the standard UBV photometric system to give response functions that yield stellar colors of standard Johnson–Morgan photometry (Johnson and Morgan 1953) as accurately as possible. It has been found (e.g., Hayes 1975; Azusienis and Straizys 1969; Buser 1978) that the response function presented by Johnson (1965) is not accurate enough to reproduce observed broadband colors in the standard system. The most accurate response functions known to date are those given by Azusienis and Straizys (1969) for the B and V bands and by Buser (1978) for the U band. Straizys, Sudzius, and Kuriliene

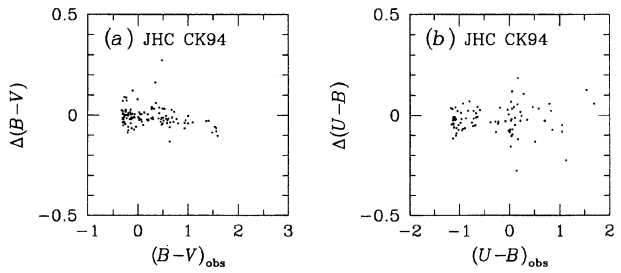

FIG. 2—(a) Difference of synthetic and observed colors $\Delta(B-V)=(B-V)_{syn}-(B-V)_{obs}$ plotted as a function of observed $B-V$ color. Stellar data are taken from Jacoby et al. (1984) and the α Lyr SED used for this synthetic calculation is CK94. (b) As (a), but for $(U-B)$ color.

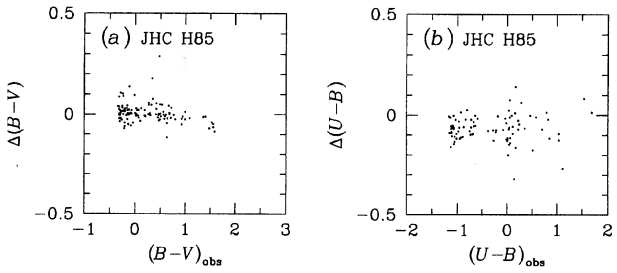

FIG. 3—As for Fig. 2, but H85 SED is used for α Lyr.

(1976) and Buser and Kurucz (1978) have argued that the set of response functions (U_3, B_2, V) reproduces the relative stellar colors of the Johnson–Morgan photometry most accurately. For redder colors we consider both Cousins' system (Cousins 1978) and Johnson's (1965). The response function of the former is taken from Bessell (1990), which reproduces Cousins' photometry most accurately.

Whether the combined use of these response functions and the SED of α Lyr provides an accurate zero point is a nontrivial problem, since the SED of α Lyr contains many strong absorption features whereas the SED was accurately measured only in the continuum part, avoiding absorption features (e.g., Oke and Schild 1970; Hayes and Latham 1975; Oke and Gunn 1983). Therefore, in most of the synthetic studies, only relative colors have been considered and they are converted into observed colors by adding an appropriate constant, as $(B-V)_{obs}=(B-V)_{syn}+a_{B-V}$ etc. An exception is a synthetic study of Gunn and Stryker (1982), in which a zero point was derived with the aid of AB79 system, by using an SED of F-subdwarf BD+17°4708 and three other F dwarfs, which were calibrated against the absolute SED of α Lyr. Since then, much effort has been invested to improve the SED of α Lyr. Here, we use the α Lyr SED to obtain directly the zero point. The most recent summary of observed SED has been given by H85, and the most recent work using the stellar atmosphere model has been given by CK94. As CK94 have discussed, the agreement between the two seems excellent except for around the Balmer absorption

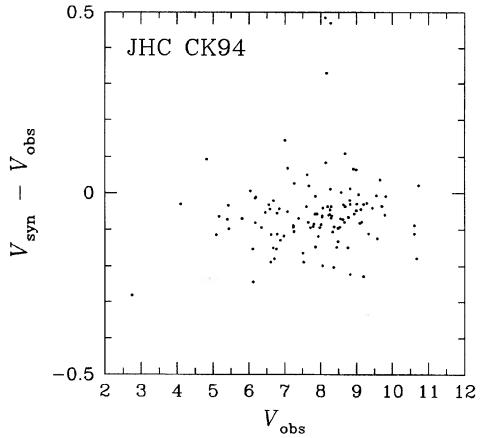

FIG. 4—Difference of synthetic and observed V magnitudes as a function of V_{obs}. Stellar data are taken from Jacoby et al. (1984) and the α Lyr SED used for this synthetic calculation is CK94.

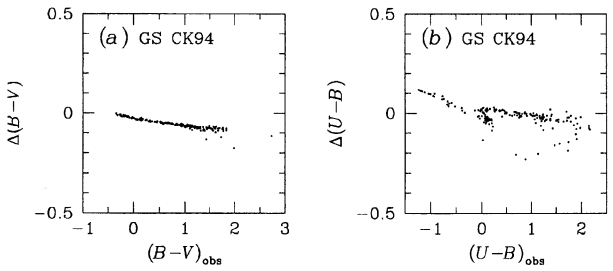

FIG. 5—As for Fig. 2, but for stars of Gunn and Stryker (1982). CK94 SED is used for α Lyr.

lines and the Paschen region (see Fig. 5 of CK94). In order to demonstrate clearly where the two disagree, we give in Fig. 1 a plot of the two SED's in terms of f_λ with an enlarged wavelength scale. This shows that absorption features of the Balmer lines are clearly different between the two: the observed SED shows dips much shallower than are predicted by an atmosphere model. We can imagine a number of possible origins for this disagreement, but we cannot determine which is correct.

For this reason, we try to use both SED's to calculate the broadband colors and examine which gives observed colors more accurately. Since the SED of H85 does not fully cover UV or IR wavelengths, we supplement it with CK94 for the ranges 3000–3300 Å and 10,500–12,000 Å , normalizing the latter to H85. We calculate the synthetic magnitude in a way such that

$$m=-2.5\left[\log\int d\lambda R(\lambda)f_\lambda-\log\int d\lambda R(\lambda)f_\lambda(\alpha\ \mathrm{Lyr})\right], \quad (1)$$

where $R(\lambda)$ is a response function and f_λ is a flux. We interpolate the response function quadratically and the flux linearly through the points given in the table, and integrate $R(\lambda)f_\lambda$ over $d\lambda$ with a 1 Å mesh. When relevant, the absolute normalization is set using the H85 zero point: $f_\lambda(\alpha\ \mathrm{Lyr})=3.44\pm0.05\times10^{-9}$erg cm^{-2} s^{-1} Å^{-1} at 5556 Å, which is compared to 3.36×10^{-9} of Oke and Schild (1970) and 3.39×10^{-9} of Hayes and Latham (1975) and of Oke and Gunn (1983).[1] Fiducial normalizations adopted by other authors are scaled to the H85 zero point.

A comparison of synthetic versus observed broadband magnitudes is shown with the stars of Jacoby et al. (1984) in Fig. 2 (using CK94) and Fig. 3 (using H85), where $\Delta(B-V)=(B-V)_{\rm syn}-(B-V)_{\rm obs}$ or $\Delta(U-B)=(U-B)_{\rm syn}-(U-B)_{\rm obs}$ is plotted as a function of the $B-V$ or $U-B$ color. Since Jacoby et al. have given SED only to 3500 Å, we extrapolate their UV SED to 3000 Å. The result is insensitive to the detail of this procedure, because the response function is already suppressed and also the flux of stars is small in the relevant wavelength range. We note that $B-V=0$ and $U-B=-0.01$ for α Lyr in the standard Johnson–Morgan system. We do not see systematic trends

TABLE 1
Synthetic vs. Observed Broad Band Colors of Galaxies

galaxy	type	T(RC3)	$(U-B)_{\rm syn}$	$(U-B)_{\rm obs}$	$(B-V)_{\rm syn}$	$(B-V)_{\rm obs}$
NGC4649	E	−5	0.77		1.02	0.97
NGC3379	E	−5	0.51	0.53	0.90	0.96
NGC4472	E	−5	0.51	0.55	0.95	0.96
NGC4648	E	−5	0.51	0.52	0.87	0.92
NGC4889*	E	−4	0.57	0.52	0.84	1.04
NGC3245	S0	−2	0.42	0.47	0.91	0.91
NGC3941	S0	−2	0.44	0.44	0.77	0.91
NGC4262	S0	−3	0.43	0.51	0.84	0.94
NGC5866	S0	−1	0.38	0.38	0.89	0.85
NGC1357	Sab	2	0.30	0.25	0.76	0.87
NGC2775	Sab	2	0.39	0.38	0.83	0.90
NGC3368	Sab	2	0.38	0.31	0.83	0.86
NGC3623	Sab	1	0.47	0.45	0.85	0.92
NGC1832	Sb	4	0.04	−0.01	0.59	0.63
NGC3147	Sb	4	0.25		0.67	0.82
NGC3627	Sb	3	0.11	0.20	0.63	0.73
NGC2903	Sbc	4	0.05	0.06	0.65	0.67
NGC5248	Sbc	4	0.04	0.05	0.64	0.65
NGC6217*	Sbc	4	−0.01	−0.18	0.48	0.63
NGC2276	Sc	5	−0.22	−0.09	0.42	0.52
NGC4775*	Sc	7	−0.28		0.29	
NGC4631*	Sc	7	−0.29		0.29	0.56
NGC6181	Sc	5	−0.05	−0.03	0.57	0.63
NGC6643	Sc	5	0.04	−0.04	0.51	0.64
NGC4449	Im	10	−0.40	−0.35	0.26	0.41
NGC4485	Im	10	−0.32	−0.22	0.28	0.39

Note — Galaxies flagged with an asterisk are not used to make a composite SED.

in any of figures. The average and scatter are $\langle\Delta(B-V)\rangle=-0.008\pm0.050$ and $\langle\Delta(U-B)\rangle=-0.012\pm0.068$ with the CK94 SED (Fig. 2), and 0.008 ± 0.050 and -0.057 ± 0.068 with H85 (Fig. 3). Here we exclude one point which gives an offset larger than >0.5 mag.

We also compare synthetic V magnitude with observed V magnitude in Fig. 4 (with CK94 SED). We obtain $\langle V_{\rm syn}-V_{\rm obs}\rangle=-0.054\pm0.108$ (for 114 stars). If the H85 SED is used the offset and scatter become -0.056 ± 0.108.

A similar analysis is also made with the Gunn and Stryker (1982) stars using CK94 SED for α Lyr (Fig. 5). Some systematic trends are visible in both $\Delta(B-V)$ and $\Delta(U-B)$ due to a small scatter of the data. The plots indicate $(B-V)_{\rm syn}=0.964(B-V)_{\rm obs}-0.026$, and $(U-B)_{\rm syn}=0.964(U-B)_{\rm obs}+0.031$ (for $U-B>0$) or $(U-B)_{\rm syn}=0.879(U-B)_{\rm obs}-0.016$ (for $U-B<0$). The variation, however, is small ($\Delta\approx0.1$) for a wide interval of colors, and is not important for our study below. If the coefficient is set

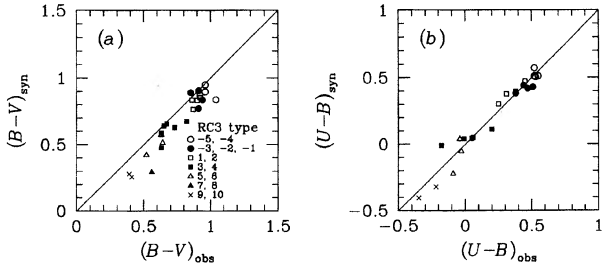

FIG. 6—(a) Regression plot of synthetic color $(B-V)_{\rm syn}$ vs. observed color $(B-V)_{\rm obs}$ for galaxies obtained by K92. The observed color is taken from RC3. Morphological-type indices are those defined in RC3. The line shows an identical regression. (b) As (a) but for $U-B$ colors.

[1]Oke and Gunn claimed that they have adopted the zero point of Oke and Schild at 5480 Å. The actual Oke and Gunn's zero point, however, is in the middle of Hayes and Latham's and Oke and Schild's. At 5556 Å Oke and Gunn's flux is closer to Hayes and Latham's, than Oke and Schild's flux.

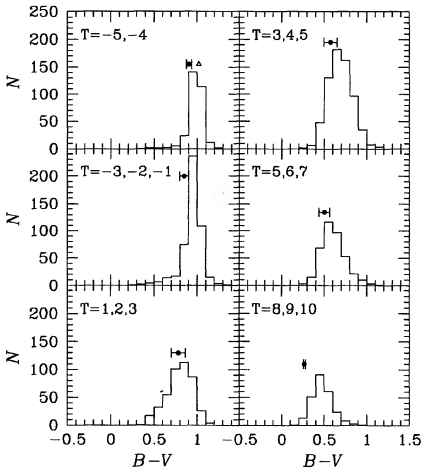

FIG. 7—$B-V$ color distribution of RC3 galaxies with specified morphological types. Only galaxies with galactic latitude $|b|>30°$ are plotted. The indicated ranges are synthetic $B-V$ colors for K92 galaxies (the range is one standard deviation). The triangle is synthetic color of NGC 4649 of Bertola et al. (1982).

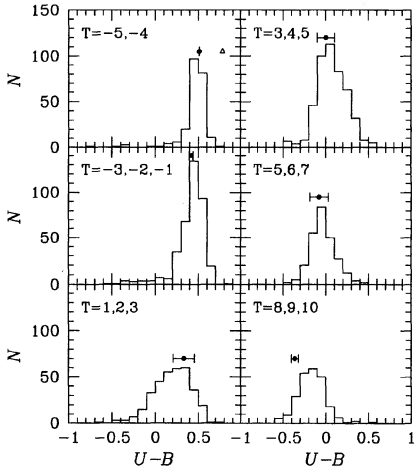

FIG. 8—As Fig. 7, but for $U-B$ color.

to be unity, the average offset is $\langle\Delta(B-V)\rangle = -0.056\pm0.026$ and $\Delta(U-B)=-0.002\ \pm0.061$. If we use the H85 SED, these numbers become -0.040 ± 0.026 and -0.046 ± 0.061, respectively.

We conclude that the error and systematic effects between synthetic and observed colors are of the order of 0.05 mag. This level of errors is acceptable for our purpose. In what follows, we take the CK94 SED (the normalization is H85), which yields a slightly smaller offset for the standard broadband colors of stars. With this SED we have

$$U=-2.5\ \log\int d\lambda R_U(\lambda)f_\lambda-14.08+c_U\,, \tag{2}$$

$$B=-2.5\ \log\int d\lambda R_B(\lambda)f_\lambda-13.00+c_B\,, \tag{3}$$

$$V=-2.5\ \log\int d\lambda R_V(\lambda)f_\lambda-13.76+c_V\,, \tag{4}$$

where the peak of the response function is normalized to unity, and c represents the magnitude of α Lyr; $c_U=0.02$, $c_B=c_V=0.03$ (Johnson and Morgan 1953).

It is desirable to carry out a similar analysis for redder bands. Unfortunately, systematic broadband photometric data are not available for the stars of Jacoby et al. (1984) and of Gunn and Stryker (1982) in R and I bands. With the CK94 SED and H85 zero point we have

TABLE 2
Average Colors of Galaxies

type	T(RC3)	n_{UB}	$\langle U-B\rangle_{obs}$	$\langle U-B\rangle_{syn}$	n_{BV}	$\langle B-V\rangle_{obs}$	$\langle B-V\rangle_{syn}$
E	−5 - −4	227	0.45 ± 0.17	0.51 ± 0.00	307	0.97 ± 0.10	0.91 ± 0.03
E(N4649)	−5			0.77		0.97	1.02
S0	−3 - −1	379	0.40 ± 0.18	0.42 ± 0.02	483	0.93 ± 0.12	0.85 ± 0.05
Sa-Sb	1 - 3	338	0.19 ± 0.21	0.33 ± 0.12	437	0.79 ± 0.15	0.78 ± 0.08
Sb-Sc	3 - 5	469	0.07 ± 0.18	0.00 ± 0.10	676	0.68 ± 0.14	0.57 ± 0.08
Sc-Sd	5 - 7	261	−0.04 ± 0.15	−0.08 ± 0.11	389	0.60 ± 0.14	0.50 ± 0.06
Sdm-Im	8 - 10	234	−0.17 ± 0.16	−0.36 ± 0.04	253	0.47 ± 0.13	0.27 ± 0.01

Notes — n_{UB} and n_{BV} are the numbers of RC3 galaxies used to obtain $\langle U-B\rangle_{obs}$ and $\langle B-V\rangle_{obs}$, respectively. Colours of NGC4649 (SED is taken from BCO) are added for comparison.

$$R_C=-2.5\ \log\int d\lambda R_{R_C}(\lambda)f_\lambda-13.67+c_{R_C}, \tag{5}$$

$$I_C=-2.5\ \log\int d\lambda R_{I_C}(\lambda)f_\lambda-14.45+c_{I_C} \tag{6}$$

for the Cousins system ($c_{R_C}=0.03$, $c_{I_C}=0.024$) (Taylor 1986), and

$$R_J=-2.5\ \log\int d\lambda R_{R_J}(\lambda)f_\lambda-13.54+c_{R_J}, \tag{7}$$

$$I_J=-2.5\ \log\int d\lambda R_{I_J}(\lambda)f_\lambda-14.18+c_{I_J} \tag{8}$$

for the Johnson red color bands ($c_{R_J}=0.07$, $c_{I_J}=0.09$) (Johnson 1965).

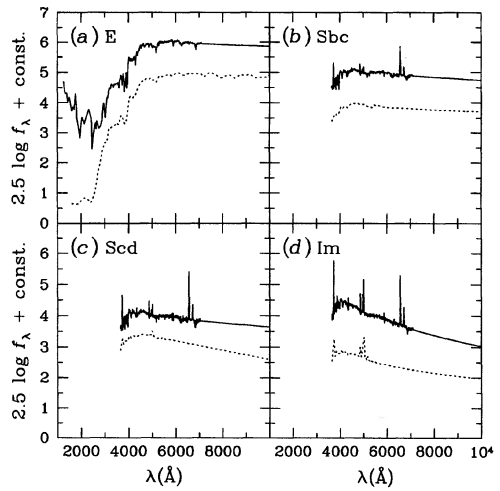

FIG. 9—Comparison of SED obtained from K92 (and Bertola et al. 1982 for elliptical galaxies) (solid curve) with the SED of Coleman et al. (1980) (dotted curve). The line for K92 SED extended to the right shows our extrapolation. Vertical axis is in arbitrary units. (a) E galaxies, (b) Sbc galaxies, (c) Scd galaxies, and (d) Im galaxies.

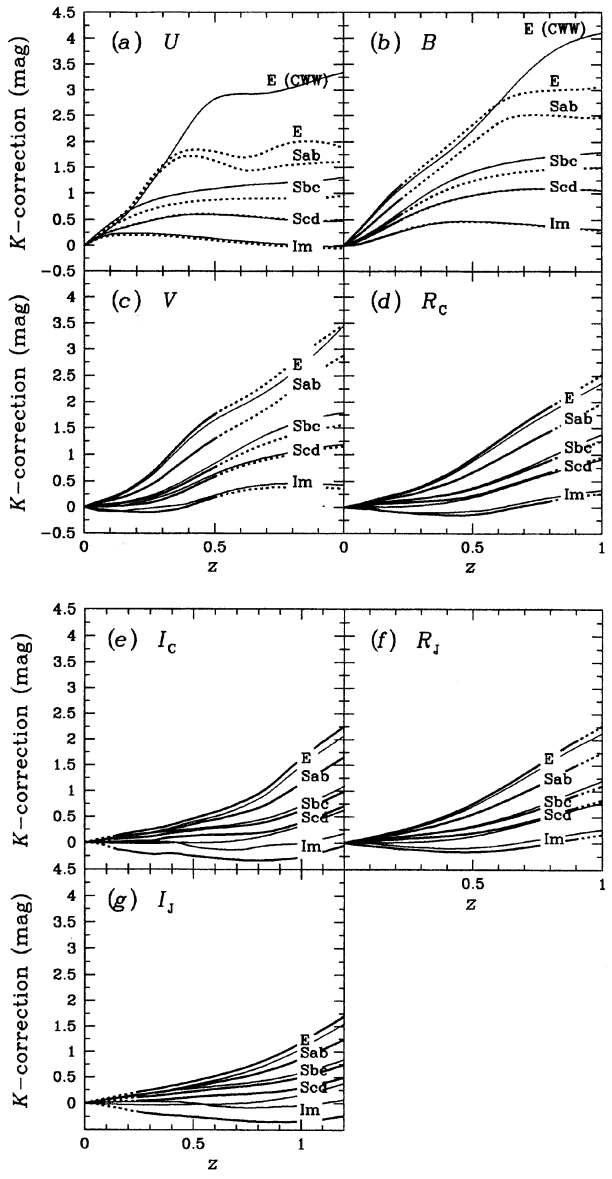

FIG. 10— K corrections derived from K92 (and Bertola et al. for E galaxies) (thick curve), as compared with those of CWW (thin curve). Solid curve segment is the portion where SED of K92 galaxies dominate the behavior. The dashed parts are determined with the UV SED of Bertola et al. (1982) (for E) or of Coleman et al. (1980) (for Sab and later types). (a)–(g) refer to 7 standard colors.

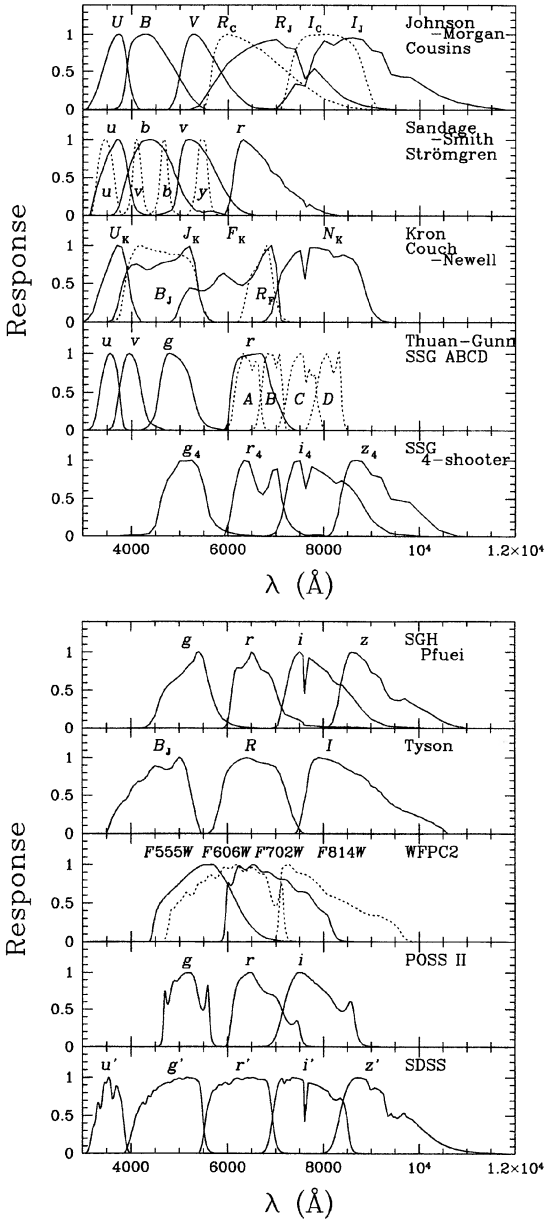

FIG. 11—48 response functions used in our study. The four response functions of Strömgren are also added. The peak height is normalized to unity. Details are given in Table 9.

3. GALAXY COLORS

A number of studies have been made to obtain the integral SED of elliptical galaxies (Schild and Oke 1971; Whitford 1971; Oke, Bertola, and Capaccioli 1981; Bertola, Capaccioli, and Oke 1982). On the other hand, available work is limited for spiral galaxies. The work of Wells (1972) has long been used to estimate the K correction of spiral galaxies (Pence 1976; Coleman, Wu, and Weedman 1980). We note that the composite SED of Coleman et al., which has been used for many studies that require galaxy colors, is based on only a handful of galaxy SEDs. Turnrose (1976) has also obtained SED of 7 Sbc and Sc galaxies. More recently, Kennicutt (1992; hereafter referred to as K92) has presented integrated SEDs for 8 early-type galaxies and 17 spiral to irregular galaxies from 3650 to 7100 Å with a resolution of 5-8 Å. This represents the largest spectrophotometric atlas available to date.

We first examine the colors obtained synthetically against those from broadband photometry. The data for the latter are taken from *Third Reference Catalogue of Bright Galaxies* (de Vaucouleurs et al. 1991, hereafter referred to as RC3). Synthetic colors are obtained in the same way as that for stellar colors in Sec. 2. The Johnson–Morgan standard photometric

TABLE 3

Galaxy Colors in Various Photometric Band Systems

(a) Standard Johnson-Morgan/Cousins (A0V)

type	$U-B$	$B-V$	$V-R_C$	R_C-I_C	$V-R_J$	R_J-I_J
E	0.64	0.96	0.61	0.70	0.71	0.73
S0	0.42	0.85	0.54	0.61	0.63	0.63
Sab	0.33	0.78	0.56	0.65	0.66	0.68
Sbc	0.00	0.57	0.52	0.62	0.60	0.65
Scd	−0.08	0.50	0.50	0.57	0.57	0.60
Im	−0.35	0.27	0.31	0.33	0.34	0.33

(b) Johnson vs. Cousins in red bandpasses

type	R_J-R_C	I_J-I_C
E	−0.11	−0.14
S0	−0.08	−0.11
Sab	−0.09	−0.12
Sbc	−0.09	−0.12
Scd	−0.08	−0.10
Im	−0.03	−0.03

(c) Sandage-Smith vs. standard colours (Jonson-Morgan/Johnson)

type	$u-U$	$b-B$	$v-V$	$r-R_C$
E	−0.01	−0.03	0.06	−0.05
S0	0.00	−0.03	0.05	−0.04
Sab	0.00	−0.02	0.05	−0.05
Sbc	0.00	−0.02	0.04	−0.05
Scd	0.00	−0.02	0.04	−0.05
Im	0.00	−0.01	0.02	−0.03

(d) Kron (Johnson-Morgan/Cousins)

type	U_K-J_K	J_K-F_K	F_K-N_K	U_K-U	J_K-B	F_K-R_C	N_K-I_C
E	0.84	1.14	0.89	0.01	−0.19	0.24	0.06
S0	0.59	1.02	0.78	0.01	−0.16	0.22	0.05
Sab	0.49	0.98	0.83	0.01	−0.14	0.23	0.05
Sbc	0.12	0.78	0.77	0.01	−0.10	0.20	0.05
Scd	0.02	0.72	0.71	0.01	−0.09	0.19	0.05
Im	−0.27	0.40	0.41	0.02	−0.06	0.12	0.03

(e) Couch-Newell (Johnson-Morgan/Cousins)

type	B_J-R_F	B_J-B	R_F-R_C
E	1.53	−0.16	−0.11
S0	1.37	−0.13	−0.10
Sab	1.34	−0.12	−0.11
Sbc	1.14	−0.08	−0.13
Scd	1.08	−0.07	−0.15
Im	0.67	−0.04	−0.13

(f) Thuan-Gunn (BD+17°4708)

type	$u-v$	$v-g$	$g-r$	$u-U$	$v-B$	$g-V$	$r-R_C$
E	0.23	0.88	0.49	−0.23	0.18	0.26	0.37
S0	0.16	0.66	0.40	−0.23	0.03	0.23	0.37
Sab	0.19	0.53	0.39	−0.19	−0.05	0.20	0.38
Sbc	0.08	0.18	0.28	−0.19	−0.27	0.13	0.36
Scd	0.04	0.09	0.25	−0.20	−0.31	0.10	0.35
Im	−0.11	−0.17	−0.06	−0.22	−0.47	−0.03	0.34

(g) Schneider, Schmidt & Gunn: 4-shooter (BD+17°4708)

type	g_4-r_4	r_4-i_4	i_4-z_4	g_4-B	g_4-V	r_4-R_C	i_4-I_C	z_4-I_C
E	0.43	0.32	0.25	−0.79	0.18	0.35	0.73	0.48
S0	0.34	0.24	0.20	−0.69	0.16	0.36	0.73	0.53
Sab	0.35	0.28	0.22	−0.64	0.15	0.36	0.73	0.51
Sbc	0.26	0.24	0.22	−0.47	0.10	0.36	0.73	0.52
Scd	0.23	0.19	0.20	−0.42	0.09	0.35	0.73	0.54
Im	−0.06	−0.03	0.07	−0.26	0.00	0.37	0.73	0.66

(h) Schneider, Gunn & Hoessel: Pfuei (BD+17°4708)

type	$g-r$	$r-i$	$i-z$	$g-B$	$g-V$	$r-R_C$	$i-I_C$	$z-I_C$
E	0.40	0.30	0.26	−0.83	0.14	0.34	0.75	0.49
S0	0.31	0.22	0.21	−0.73	0.12	0.35	0.75	0.53
Sab	0.33	0.26	0.23	−0.67	0.12	0.35	0.75	0.51
Sbc	0.26	0.21	0.23	−0.49	0.09	0.34	0.75	0.52
Scd	0.24	0.16	0.21	−0.43	0.08	0.33	0.75	0.54
Im	−0.02	−0.06	0.07	−0.25	0.02	0.35	0.73	0.66

(i) Schneider, Schmidt & Gunn: red narrow bands (AB)

type	$A-B$	$B-C$	$C-D$	$A-R_C$	$B-R_C$	$C-I_C$	$D-I_C$
E	0.15	0.21	0.13	0.20	0.06	0.55	0.42
S0	0.11	0.15	0.12	0.19	0.08	0.54	0.42
Sab	0.14	0.17	0.13	0.20	0.07	0.55	0.42
Sbc	0.08	0.16	0.13	0.17	0.09	0.55	0.42
Scd	0.03	0.14	0.12	0.14	0.11	0.54	0.42
Im	−0.06	0.03	0.04	0.11	0.17	0.47	0.43

(j) Tyson (CCD) (Landolt)

type	B_J-R	$R-I$	B_J-B	$R-R_C$	$I-I_C$
E	1.38	0.86	−0.22	−0.03	−0.18
S0	1.24	0.74	−0.18	−0.03	−0.16
Sab	1.21	0.79	−0.16	−0.03	−0.17
Sbc	1.01	0.75	−0.12	−0.03	−0.17
Scd	0.94	0.69	−0.10	−0.04	−0.16
Im	0.53	0.38	−0.07	−0.03	−0.09

(k) WFPC2 (Holzman et al.)

type	F555W−F606W	F606W−F702W	F702W−F814W	F555W $-V$	F606W $-V$	F702W $-R_C$	F814W $-I_C$
E	0.33	0.47	0.47	0.00	−0.33	−0.19	0.04
S0	0.30	0.41	0.41	0.01	−0.29	−0.16	0.04
Sab	0.31	0.44	0.44	0.00	−0.30	−0.18	0.04
Sbc	0.28	0.40	0.41	0.00	−0.28	−0.17	0.04
Scd	0.27	0.38	0.37	−0.01	−0.28	−0.16	0.04
Im	0.17	0.22	0.20	−0.01	−0.18	−0.09	0.04

(l) POSS II (BD+17°4708)

type	$g_{POSS}-r_{POSS}$	$r_{POSS}-i_{POSS}$	$g_{POSS}-B$	$g_{POSS}-V$	$r_{POSS}-R_C$	$i_{POSS}-I_C$
E	0.44	0.26	−0.79	0.17	0.34	0.78
S0	0.35	0.19	−0.69	0.16	0.35	0.77
Sab	0.37	0.23	−0.63	0.15	0.35	0.77
Sbc	0.28	0.19	−0.47	0.11	0.34	0.77
Scd	0.25	0.14	−0.41	0.09	0.34	0.77
Im	−0.04	−0.05	−0.26	0.01	0.36	0.74

(m) SDSS (AB)

type	$u'-g'$	$g'-r'$	$r'-i'$	$i'-z'$	$u'-U$	$g'-B$	$r'-R_C$	$i'-I_C$	$z'-I_C$
E	1.99	0.77	0.43	0.36	0.80	−0.55	0.25	0.53	0.16
S0	1.70	0.68	0.34	0.29	0.80	−0.49	0.23	0.51	0.21
Sab	1.60	0.66	0.38	0.32	0.82	−0.45	0.24	0.51	0.19
Sbc	1.16	0.52	0.33	0.32	0.82	−0.34	0.23	0.51	0.20
Scd	1.04	0.48	0.28	0.29	0.81	−0.30	0.22	0.51	0.22
Im	0.64	0.20	0.04	0.11	0.78	−0.21	0.17	0.46	0.35

Note — Denoted in parentheses are the adopted zero point.

system is used together with CK94 SED for α Lyr.

In Table 1 we compare the synthetically obtained colors with those listed in RC3 for $B-V$ and $U-B$ for galaxies measured by K92. We also add from Bertola et al. (1982) the colors for NGC 4649, which represents a typical galaxy that shows a strong UV component shortward of 2500 Å. Regression diagrams are given in Fig. 6. Since the SED of K92 is limited to longward of 3650 Å, we extrapolated the flux of each galaxy to the UV side using the SED of Coleman et al. (or of NGC 4649 for E and S0) with the normalization adjusted at 3650–3700 Å. For elliptical galaxies the UV SED of Coleman et al. represents a UV quiscent galaxy. Therefore, we expect general UV SED between the two. For our calculation of U colors of nearby galaxies, however, the extrapolation is only slight, and the result does not depend upon whichever UV SED is used for the extrapolation. The Galactic reddening corrections are not made for the colors (when the original data include corrections, we removed them). We see that the agreement is generally good; the offset is typically smaller than 0.1 mag for most of the galaxies. There is, however, a trend that synthetic $B-V$ colors are slightly bluer; there are a few cases where the difference of the two colors is as large as 0.2 mag. This might be ascribed to the difference of the aperture for broadband photometry and for spectrophotometry, as well as errors of the measurements. When an offset of one of the colors is larger than 0.15 mag, we exclude those galaxies from the averaging procedure which will be employed later in the present work.

The next question to ask is whether the galaxies studied by K92 represent a typical member of each morphological type. We show in Fig. 7 the $B-V$ color distribution of galaxies in RC3, by grouping them into 6 morphological types (E, S0, Sa-Sb, Sb-Sc, Sc-Sd, Sdm-Im, allowing for overlaps). We also indicate colors from synthetic calculation obtained

TABLE 4
Magnitudes of α Lyr in the Thuan–Gunn Definition of the Zero Point

U	B	V	R_C	I_C	R_J	I_J
−0.181	−0.342	0.083	0.399	0.752	0.473	0.805

U_K	J_K	F_K	N_K	B_J	R_F
−0.195	−0.256	0.271	0.723	−0.281	0.481

u	v	g	r	g_4	r_4	i_4	z_4
0.000	−0.440	−0.126	0.429	−0.047	0.455	0.739	0.851

g	r	i	z	A	B	C	D
−0.016	0.458	0.730	0.853	0.404	0.525	0.664	0.770

F555W	F606W	F702W	F814W	g_{POSS}	r_{POSS}	i_{POSS}
0.069	0.250	0.511	0.726	−0.035	0.459	0.709

u'	g'	r'	i'	z'
−0.077	−0.178	0.342	0.687	0.855

TABLE 5
AB Magnitudes of α Lyr

U	B	V	R_C	I_C	R_J	I_J
0.710	−0.110	0.011	0.199	0.456	0.249	0.504

U_K	J_K	F_K	N_K	B_J	R_F
0.689	−0.056	0.120	0.434	−0.091	0.259

u	v	g	r	g_4	r_4	i_4	z_4
1.049	0.041	−0.075	0.221	−0.043	0.236	0.445	0.545

g	r	i	z	A	B	C	D
−0.031	0.241	0.437	0.547	0.210	0.276	0.380	0.471

F555W	F606W	F702W	F814W	g_{POSS}	r_{POSS}	i_{POSS}
0.009	0.111	0.275	0.434	−0.034	0.244	0.424

u'	g'	r'	i'	z'
0.928	−0.087	0.163	0.401	0.549

by averaging the K92 galaxies and NGC 4649 of Bertola et al. We use only galaxies at Galactic latitude $|b|>30°$ and do not apply reddening corrections. The number of galaxies used to draw this histogram and the average colors are also given in Table 2. Figure 7 shows that the averages of synthetic colors of the galaxies studied by K92, except for those for the latest type Sdm-Im, reside close to the median of the color distribution of the RC3 galaxies, with a trend that the former is slightly ($\leq$0.1) bluer. This does not necessarily mean that the galaxies in the K92 sample are bluer than the average, but it probably reflects the fact that synthetic colors are slightly bluer than observed broadband colors. For Sdm-Im synthetic magnitudes are significantly bluer ($\approx$0.2 mag). This is due to the fact that the two galaxies NGC 4449 and NGC 4485 are among the bluest nearby galaxies. Also noteworthy in this figure is the fact that the color distribution

TABLE 6
Galaxy Colors at $z=0.2$

(a) Standard Johnson-Morgan/Cousins

type	$U-B$	$B-V$	$V-R_C$	R_C-I_C	$V-R_J$	R_J-I_J
E	0.47	1.59	0.80	0.77	0.93	0.78
S0	0.41	1.38	0.71	0.70	0.83	0.68
Sab	0.38	1.30	0.67	0.71	0.79	0.72
Sbc	0.07	0.98	0.52	0.66	0.63	0.66
Scd	−0.10	0.89	0.47	0.63	0.57	0.63
Im	−0.39	0.61	0.30	0.40	0.34	0.36
E(CWW)	0.43	1.59	0.82	0.81	0.96	0.80

(b) Kron

type	U_K-J_K	J_K-F_K	F_K-N_K	U_K-U	J_K-B	F_K-R_C	N_K-I_C
E	0.86	1.72	1.00	0.01	−0.39	0.29	0.05
S0	0.75	1.51	0.91	0.01	−0.33	0.25	0.05
Sab	0.71	1.41	0.91	0.01	−0.31	0.25	0.05
Sbc	0.32	1.07	0.81	0.02	−0.23	0.20	0.05
Scd	0.13	0.96	0.78	0.02	−0.21	0.19	0.05
Im	−0.22	0.63	0.49	0.02	−0.15	0.13	0.03
E(CWW)	0.82	1.72	1.05	0.01	−0.38	0.30	0.06

(c) Couch-Newell

type	B_J-R_F	B_J-B	R_F-R_C
E	2.26	−0.31	−0.18
S0	2.01	−0.26	−0.18
Sab	1.89	−0.24	−0.16
Sbc	1.46	−0.18	−0.13
Scd	1.32	−0.16	−0.12
Im	0.87	−0.11	−0.07
E(CWW)	2.27	−0.30	−0.16

(d) Schneider, Schmidt & Gunn: 4-shooter

type	g_4-r_4	r_4-i_4	i_4-z_4	g_4-B	g_4-V	r_4-R_C	i_4-I_C	z_4-I_C
E	0.86	0.36	0.26	−1.21	0.38	0.32	0.73	0.47
S0	0.71	0.29	0.20	−1.07	0.32	0.32	0.73	0.53
Sab	0.62	0.31	0.23	−1.02	0.28	0.33	0.73	0.50
Sbc	0.35	0.27	0.20	−0.81	0.17	0.35	0.73	0.53
Scd	0.26	0.26	0.16	−0.75	0.15	0.36	0.73	0.58
Im	−0.04	0.07	0.00	−0.55	0.06	0.40	0.73	0.73
E(CWW)	0.88	0.41	0.23	−1.20	0.39	0.33	0.73	0.50

(e) Schneider, Gunn & Hoessel: Pfuei

type	$g-r$	$r-i$	$i-z$	$g-B$	$g-V$	$r-R_C$	$i-I_C$	$z-I_C$
E	0.76	0.34	0.27	−1.31	0.28	0.32	0.75	0.47
S0	0.63	0.27	0.21	−1.15	0.23	0.32	0.74	0.53
Sab	0.55	0.29	0.25	−1.09	0.21	0.33	0.75	0.50
Sbc	0.32	0.26	0.21	−0.84	0.14	0.35	0.74	0.54
Scd	0.23	0.25	0.16	−0.77	0.12	0.36	0.74	0.58
Im	−0.04	0.07	−0.01	−0.55	0.06	0.40	0.73	0.74
E(CWW)	0.78	0.38	0.25	−1.30	0.28	0.32	0.75	0.50

(f) Tyson

type	B_J-R	$R-I$	B_J-B	$R-R_C$	$I-I_C$
E	2.09	0.91	−0.34	−0.05	−0.19
S0	1.84	0.81	−0.30	−0.05	−0.16
Sab	1.71	0.85	−0.30	−0.05	−0.18
Sbc	1.30	0.79	−0.24	−0.03	−0.17
Scd	1.16	0.76	−0.23	−0.03	−0.15
Im	0.75	0.46	−0.17	−0.02	−0.07
E(CWW)	2.11	0.95	−0.34	−0.04	−0.18

(g) WFPC2

type	F555W −F606W	F606W −F702W	F702W −F814W	F555W $-V$	F606W $-V$	F702W $-R_C$	F814W $-I_C$
E	0.49	0.58	0.51	0.04	−0.45	−0.23	0.03
S0	0.44	0.53	0.45	0.05	−0.40	−0.21	0.03
Sab	0.41	0.51	0.47	0.05	−0.37	−0.21	0.03
Sbc	0.32	0.43	0.43	0.04	−0.28	−0.19	0.04
Scd	0.28	0.40	0.41	0.04	−0.25	−0.18	0.04
Im	0.18	0.25	0.25	0.02	−0.15	−0.11	0.05
E(CWW)	0.50	0.60	0.53	0.04	−0.46	−0.24	0.04

(h) POSS II

type	$g_{POSS}-r_{POSS}$	$r_{POSS}-i_{POSS}$	$g_{POSS}-B$	$g_{POSS}-V$	$r_{POSS}-R_C$	$i_{POSS}-I_C$
E	0.85	0.30	−1.23	0.36	0.31	0.78
S0	0.69	0.24	−1.09	0.29	0.31	0.77
Sab	0.60	0.26	−1.05	0.25	0.32	0.77
Sbc	0.33	0.23	−0.83	0.15	0.34	0.77
Scd	0.24	0.23	−0.77	0.12	0.36	0.76
Im	−0.05	0.07	−0.56	0.05	0.40	0.73
E(CWW)	0.87	0.34	−1.22	0.36	0.31	0.78

(i) SDSS

type	$u'-g'$	$g'-r'$	$r'-i'$	$i'-z'$	$u'-U$	$g'-B$	$r'-R_C$	$i'-I_C$	$z'-I_C$
E	2.19	1.31	0.52	0.37	0.91	−0.80	0.27	0.52	0.15
S0	2.05	1.13	0.45	0.29	0.92	−0.71	0.26	0.50	0.21
Sab	1.96	1.02	0.46	0.33	0.89	−0.69	0.26	0.51	0.18
Sbc	1.40	0.71	0.39	0.29	0.77	−0.55	0.24	0.50	0.22
Scd	1.17	0.62	0.37	0.24	0.76	−0.51	0.24	0.49	0.26
Im	0.71	0.32	0.15	0.02	0.72	−0.39	0.20	0.45	0.42
E(CWW)	2.12	1.33	0.56	0.35	0.90	−0.80	0.28	0.53	0.18

TABLE 7
Galaxy Colors at $z=0.5$

(a) Standard Johnson-Morgan/Cousins

type	$U-B$	$B-V$	$V-R_C$	R_C-I_C	$V-R_J$	R_J-I_J
E	0.13	1.53	1.44	1.17	1.72	1.07
S0	0.13	1.49	1.25	1.05	1.49	0.97
Sab	−0.01	1.47	1.19	0.97	1.40	0.93
Sbc	−0.31	1.05	0.93	0.75	1.06	0.74
Scd	−0.36	0.88	0.86	0.67	0.97	0.68
Im	−0.72	0.55	0.63	0.44	0.69	0.42
E(CWW)	1.26	1.53	1.44	1.18	1.72	1.10

(b) Kron

type	U_K-J_K	J_K-F_K	F_K-N_K	U_K-U	J_K-B	F_K-R_C	N_K-I_C
E	0.52	2.17	1.53	0.02	−0.37	0.42	0.06
S0	0.52	2.00	1.37	0.02	−0.37	0.38	0.06
Sab	0.36	1.95	1.28	0.02	−0.35	0.37	0.06
Sbc	−0.09	1.47	1.00	0.02	−0.20	0.31	0.05
Scd	−0.18	1.30	0.92	0.02	−0.16	0.29	0.04
Im	−0.60	0.85	0.64	0.02	−0.10	0.23	0.03
E(CWW)	1.60	2.18	1.55	0.00	−0.35	0.43	0.06

(c) Couch-Newell

type	B_J-R_F	B_J-B	R_F-R_C
E	2.98	−0.29	−0.30
S0	2.73	−0.29	−0.28
Sab	2.66	−0.27	−0.26
Sbc	2.03	−0.15	−0.20
Scd	1.81	−0.11	−0.18
Im	1.24	−0.06	−0.12
E(CWW)	2.96	−0.28	−0.28

(d) Schneider, Schmidt & Gunn: 4-shooter

type	g_4-r_4	r_4-i_4	i_4-z_4	g_4-B	g_4-V	r_4-R_C	i_4-I_C	z_4-I_C
E	1.58	0.65	0.33	−1.17	0.36	0.22	0.73	0.40
S0	1.36	0.54	0.30	−1.16	0.33	0.23	0.73	0.43
Sab	1.31	0.48	0.30	−1.12	0.35	0.24	0.73	0.43
Sbc	0.96	0.30	0.25	−0.74	0.31	0.28	0.73	0.48
Scd	0.83	0.24	0.24	−0.62	0.26	0.29	0.73	0.49
Im	0.48	0.06	0.08	−0.36	0.18	0.33	0.72	0.64
E(CWW)	1.57	0.67	0.36	−1.17	0.36	0.23	0.73	0.38

(e) Schneider, Gunn & Hoessel: Pfuei

type	$g-r$	$r-i$	$i-z$	$g-B$	$g-V$	$r-R_C$	$i-I_C$	$z-I_C$
E	1.52	0.62	0.36	−1.23	0.30	0.22	0.76	0.40
S0	1.30	0.51	0.33	−1.21	0.28	0.23	0.76	0.44
Sab	1.24	0.45	0.32	−1.19	0.28	0.24	0.76	0.44
Sbc	0.89	0.28	0.27	−0.80	0.25	0.28	0.75	0.48
Scd	0.78	0.22	0.25	−0.67	0.21	0.29	0.75	0.50
Im	0.45	0.05	0.08	−0.40	0.15	0.33	0.73	0.65
E(CWW)	1.51	0.64	0.38	−1.23	0.30	0.23	0.76	0.38

(f) Tyson

type	B_J-R	$R-I$	B_J-B	$R-R_C$	$I-I_C$
E	2.70	1.29	−0.38	−0.11	−0.23
S0	2.47	1.15	−0.38	−0.10	−0.21
Sab	2.41	1.08	−0.35	−0.10	−0.21
Sbc	1.86	0.85	−0.19	−0.08	−0.18
Scd	1.65	0.77	−0.16	−0.07	−0.17
Im	1.13	0.47	−0.10	−0.05	−0.08
E(CWW)	2.70	1.32	−0.36	−0.10	−0.25

(g) WFPC2

type	F555W −F606W	F606W −F702W	F702W −F814W	F555W $-V$	F606W $-V$	F702W $-R_C$	F814W $-I_C$
E	0.84	0.93	0.71	−0.08	−0.92	−0.41	0.04
S0	0.73	0.83	0.64	−0.06	−0.79	−0.37	0.04
Sab	0.69	0.78	0.59	−0.06	−0.75	−0.34	0.04
Sbc	0.53	0.61	0.46	−0.03	−0.56	−0.25	0.04
Scd	0.48	0.56	0.41	−0.04	−0.52	−0.22	0.04
Im	0.34	0.41	0.26	−0.03	−0.37	−0.15	0.03
E(CWW)	0.83	0.94	0.73	−0.09	−0.92	−0.42	0.03

(h) POSS II

type	$g_{POSS}-r_{POSS}$	$r_{POSS}-i_{POSS}$	$g_{POSS}-B$	$g_{POSS}-V$	$r_{POSS}-R_C$	$i_{POSS}-I_C$
E	1.59	0.55	−1.19	0.34	0.19	0.81
S0	1.36	0.46	−1.17	0.31	0.21	0.80
Sab	1.31	0.40	−1.13	0.34	0.23	0.80
Sbc	0.96	0.24	−0.74	0.31	0.27	0.78
Scd	0.83	0.19	−0.63	0.26	0.28	0.77
Im	0.47	0.04	−0.39	0.16	0.33	0.73
E(CWW)	1.58	0.57	−1.18	0.35	0.20	0.81

(i) SDSS

type	$u'-g'$	$g'-r'$	$r'-i'$	$i'-z'$	$u'-U$	$g'-B$	$r'-R_C$	$i'-I_C$	$z'-I_C$
E	1.54	1.78	1.01	0.49	0.63	−0.78	0.41	0.57	0.08
S0	1.54	1.61	0.85	0.44	0.64	−0.77	0.36	0.55	0.12
Sab	1.36	1.59	0.76	0.43	0.63	−0.74	0.33	0.55	0.12
Sbc	0.89	1.23	0.50	0.35	0.74	−0.47	0.27	0.52	0.16
Scd	0.77	1.09	0.42	0.33	0.73	−0.40	0.25	0.50	0.18
Im	0.22	0.73	0.20	0.12	0.70	−0.24	0.21	0.46	0.34
E(CWW)	2.75	1.76	1.03	0.51	0.70	−0.79	0.42	0.56	0.05

of galaxies is reasonably sharp even for spiral galaxies, if a morphology grouping is made. Figure 8 is a corresponding figure for the $U-B$ colors. Here, the colors calculated from K92 fall almost at the median of the distributions, except for Sdm-Im for the reason the same as for $B-V$. The analysis given here indicates that the composite SED obtained from galaxies of the K92 sample probably well represents a median of entire galaxy sample with the exception for Sdm-Im, for which the K92 sample represents the bluest of normal galaxies.

We now make an assessment of the SED of Coleman et al. (1980) against those of K92. In Fig. 9 we compare the composite SED of Coleman et al. (reddening correction is now included again) with that obtained from the K92 data. Here and hereafter we rename Sa-Sb as Sab, Sb-Sc as Sbc, and so on. Im represents the bluest galaxies. Corresponding to Fig. 9, we show in Fig. 10(a)–10(g) the K correction calculated from the two SED's. For early type SED, we take an average of three elliptical galaxies of K92 and NGC 4649 of Bertola et al. (1982), the quality of which seems equally good. Since the K92's SED does not go beyond 3650 Å, the UV part is supplemented with the SED of Coleman et al. (for the late types) and NGC 4649 (for the early types). The portion of the curve dominantly determined by the K92 data is shown by solid curves. We see that the agreement is good for this part, with a difference between the two being at most 0.1 mag except for Im. A larger difference becomes manifest, however, for the part for which the K correction is dominated by the UV SED. The most conspicuous difference is seen for elliptical galaxies for $z \geqslant 0.4$ in U and $z \geqslant 0.7$ in B; it arises from a strong UV component of NGC 4649, compared with very weak UV of the SED of Coleman et al.

4. TRANSFORMATION LAWS AMONG VARIOUS PHOTOMETRIC SYSTEMS

We obtain the transformation law among various colors frequently used in the literature. We take Johnson–Morgan UBV (Johnson and Morgan 1953) and Cousins R_CI_C (Cousins 1978; Bessell 1976) as a standard set. We also consider Johnson R_JI_J (Johnson 1965); Sandage–Smith $ubvr$ (Sandage and Smith 1963); Thuan–Gunn $uvgr$ (Thuan and Gunn 1976) and its CCD versions $g_4r_4i_4z_4$ (Schneider, Schmidt and Gunn 1989), $griz$ (Schneider, Gunn and Hoessel 1983); red narrowband $ABCD$ of Schneider, Schmidt, and Gunn (1991). Also often used for galaxy studies are Kron $U_KJ_KF_KN_K$ (Kron 1980; Koo 1985) and Couch–Newell B_JR_F (Couch and Newell 1980). We include in our consideration Tyson's B_JRI (Tyson 1988) and a few wide filters, $F555W$, $F606W$, $F702W$ and $F814W$, of WFPC2 on the

TABLE 8
Galaxy Colors at $z=0.8$

(a) Standard Johnson-Morgan/Cousins

type	$U-B$	$B-V$	$V-R_C$	R_C-I_C	$V-R_J$	R_J-I_J
E	−0.37	1.23	1.44	1.67	1.80	1.62
S0	−0.38	1.23	1.38	1.49	1.68	1.43
Sab	−0.62	1.10	1.35	1.43	1.65	1.34
Sbc	−0.54	0.72	0.99	1.15	1.23	1.04
Scd	−0.64	0.66	0.84	1.06	1.06	0.95
Im	−0.75	0.26	0.57	0.78	0.72	0.67
E(CWW)	0.03	2.15	1.39	1.66	1.75	1.62

(b) Kron

type	U_K-J_K	J_K-F_K	F_K-N_K	U_K-U	J_K-B	F_K-R_C	N_K-I_C
E	−0.21	1.89	2.18	0.01	−0.15	0.63	0.13
S0	−0.21	1.88	1.95	0.01	−0.15	0.57	0.11
Sab	−0.47	1.77	1.86	0.02	−0.14	0.54	0.11
Sbc	−0.38	1.18	1.46	0.02	−0.14	0.39	0.08
Scd	−0.49	1.03	1.33	0.02	−0.13	0.34	0.07
Im	−0.66	0.53	0.96	0.02	−0.07	0.23	0.05
E(CWW)	0.61	2.36	2.17	0.02	−0.55	0.63	0.12

(c) Couch-Newell

type	B_J-R_F	B_J-B	R_F-R_C
E	2.52	−0.11	−0.04
S0	2.50	−0.11	0.00
Sab	2.41	−0.09	−0.06
Sbc	1.76	−0.09	−0.14
Scd	1.54	−0.09	−0.13
Im	0.94	−0.03	−0.15
E(CWW)	3.07	−0.44	0.04

(d) Schneider, Schmidt & Gunn: 4-shooter

type	g_4-r_4	r_4-i_4	i_4-z_4	g_4-B	g_4-V	r_4-R_C	i_4-I_C	z_4-I_C
E	1.50	1.40	0.53	−0.69	0.54	0.48	0.76	0.23
S0	1.48	1.17	0.44	−0.69	0.54	0.44	0.75	0.31
Sab	1.45	1.07	0.40	−0.60	0.50	0.40	0.75	0.35
Sbc	0.86	0.73	0.26	−0.51	0.20	0.33	0.74	0.49
Scd	0.67	0.66	0.21	−0.49	0.18	0.34	0.74	0.53
Im	0.26	0.40	0.09	−0.22	0.04	0.34	0.73	0.65
E(CWW)	1.51	1.38	0.55	−1.56	0.59	0.47	0.75	0.21

(e) Schneider, Gunn & Hoessel: Pfuei

type	$g-r$	$r-i$	$i-z$	$g-B$	$g-V$	$r-R_C$	$i-I_C$	$z-I_C$
E	1.43	1.28	0.58	−0.83	0.40	0.41	0.81	0.23
S0	1.39	1.09	0.48	−0.82	0.40	0.39	0.79	0.31
Sab	1.35	1.00	0.43	−0.73	0.37	0.36	0.79	0.35
Sbc	0.84	0.71	0.28	−0.55	0.17	0.32	0.76	0.49
Scd	0.65	0.64	0.23	−0.52	0.14	0.34	0.76	0.53
Im	0.27	0.39	0.10	−0.21	0.05	0.34	0.74	0.64
E(CWW)	1.42	1.26	0.60	−1.72	0.43	0.41	0.81	0.21

(f) Tyson

type	B_J-R	$R-I$	B_J-B	$R-R_C$	$I-I_C$
E	2.48	2.11	−0.09	0.10	−0.34
S0	2.45	1.84	−0.09	0.06	−0.29
Sab	2.33	1.72	−0.08	0.03	−0.26
Sbc	1.60	1.31	−0.14	−0.03	−0.19
Scd	1.39	1.19	−0.13	−0.02	−0.16
Im	0.79	0.84	−0.07	−0.04	−0.10
E(CWW)	2.98	2.11	−0.47	0.09	−0.35

(g) WFPC2

type	F555W −F606W	F606W −F702W	F702W −F814W	F555W $-V$	F606W $-V$	F702W $-R_C$	F814W $-I_C$
E	0.68	1.12	1.14	−0.08	−0.76	−0.44	0.09
S0	0.67	1.03	1.00	−0.08	−0.75	−0.40	0.09
Sab	0.68	1.01	0.94	−0.06	−0.74	−0.40	0.08
Sbc	0.51	0.81	0.73	−0.03	−0.54	−0.35	0.07
Scd	0.44	0.72	0.67	0.01	−0.44	−0.32	0.06
Im	0.28	0.52	0.49	−0.01	−0.29	−0.25	0.05
E(CWW)	0.70	1.11	1.15	−0.03	−0.72	−0.44	0.08

(h) POSS II

type	$g_{POSS}-r_{POSS}$	$r_{POSS}-i_{POSS}$	$g_{POSS}-B$	$g_{POSS}-V$	$r_{POSS}-R_C$	$i_{POSS}-I_C$
E	1.61	1.17	−0.66	0.57	0.40	0.90
S0	1.58	0.99	−0.65	0.57	0.37	0.87
Sab	1.54	0.92	−0.56	0.54	0.34	0.85
Sbc	0.91	0.64	−0.51	0.21	0.30	0.80
Scd	0.71	0.58	−0.48	0.18	0.31	0.79
Im	0.29	0.35	−0.21	0.05	0.32	0.76
E(CWW)	1.60	1.16	−1.55	0.60	0.39	0.90

(i) SDSS

type	$u'-g'$	$g'-r'$	$r'-i'$	$i'-z'$	$u'-U$	$g'-B$	$r'-R_C$	$i'-I_C$	$z'-I_C$
E	0.73	1.76	1.47	0.84	0.73	−0.38	0.54	0.74	−0.10
S0	0.73	1.74	1.29	0.70	0.73	−0.37	0.49	0.69	−0.02
Sab	0.41	1.64	1.25	0.63	0.71	−0.33	0.48	0.66	0.03
Sbc	0.51	0.96	0.97	0.41	0.70	−0.35	0.40	0.58	0.17
Scd	0.37	0.80	0.87	0.34	0.68	−0.33	0.37	0.56	0.21
Im	0.14	0.35	0.58	0.16	0.70	−0.18	0.29	0.50	0.34
E(CWW)	1.70	1.97	1.47	0.86	0.64	−1.03	0.55	0.74	−0.12

Hubble Space Telescope (Burrows et al. 1994). We also add two more recent survey photometric systems, *gri* of the Second Palomer Sky Survey (POSS II) (Djorgovsky, private communication) and $u'g'r'i'z'$ of the Sloan Digital Sky Survey (SDSS) (Fukugita et al. 1995). The response curves are compiled in Fig. 11, and the characteristics are summarized in Appendix A. 1.0 airmass is assumed throughout our study, except for those for WFPC2. We also include the photometric band of Strömgren $uvby$ (Strömgren 1963) in this figure (the response functions are taken from Matsushima 1969 and Olson 1974).

We note that for photometric bands defined with the use of CCD we take the definition,

$$m=-2.5\log\frac{\int d\nu S(\nu)f_\nu/\nu}{\int d\nu S(\nu)/\nu}-\text{const.}, \tag{9}$$

where $S(\nu)$ is a product of the overall transmission function and the quantum efficiency of CCD, as usually adopted. An extra ν^{-1} is inserted so that the integrand is proportional to the photon number received at a detector (Gunn, private communication). On the other hand, we use an integral over $R(\lambda)$ times the flux for photoelectric (and also photographic) magnitude, since R is measured as a net response of the system.

In Table 3 we show color differences among various pho-

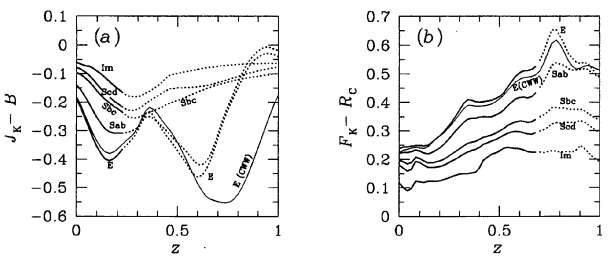

FIG. 12—Difference of the K corrections for (a) J_K-B and (b) $F-R_C$. The meaning of curves is the same as for Fig. 10.

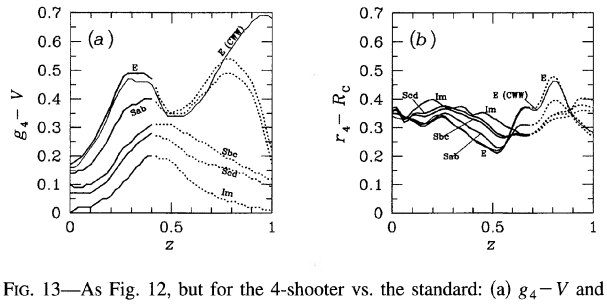

FIG. 13—As Fig. 12, but for the 4-shooter vs. the standard: (a) g_4-V and (b) r_4-R_C. Note a different definition (Thuan–Gunn definition) of the zero point for the 4-shooter photometric system.

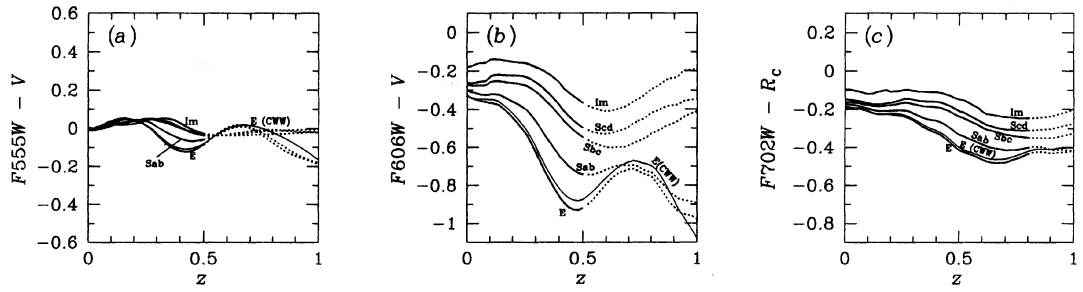

FIG. 14—As Fig. 12, but for WFPC2 vs. the standard: (a) $F555-V$, (b) $F606-V$, and (c) $F702-R_C$.

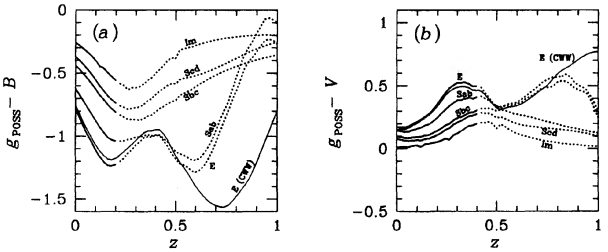

FIG. 15—As Fig. 12, but for POSS II vs. the standard: (a) $g_{\rm POSS}-B$ and (b) $g_{\rm POSS}-V$. The Thuan–Gunn definition is adopted for the zero point in POSS II.

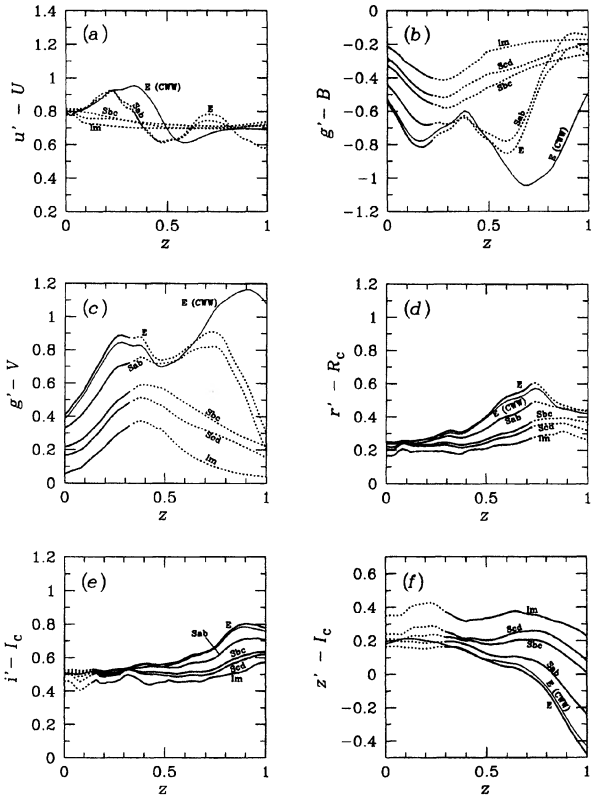

FIG. 16—As Fig. 12, but for SDSS vs. the standard: (a) $u'-U$, (b) $g'-B$, (c) $g'-V$, (d) $r'-R_C$, (e) $i'-I_C$, and (f) $z'-I_C$. The AB magnitude system is adopted in the SDSS system.

tometric bands for 6 morphology types of galaxies using the composite SED obtained from the K92 data and data of Bertola et al. (1982) as discussed in Sec. 3. Galactic reddening is not corrected for these colors. A color difference between two arbitrary bands can be obtained by arithmetically combining two or more numbers. A remark must be made on the zero point of each system. In the standard system magnitudes and colors are defined by some specific samples of stars (e.g., stars in the North Polar Sequence for V magnitude; 6 specific bright A0 V stars for $B-V$ etc.), and therefore neither magnitude nor colors is necessarily precisely zero for α Lyr. For α Lyr, $V=0.03$, $B-V=0$, $U-B=-0.01$ (Johnson and Morgan 1953), $V-Rc=0$ and $V-Ic=0.006$ (Taylor 1986; Bessell 1983). The majority of recent efforts to establish accurate brightnesses of stars have adopted these systems and calibrations (e.g., Landolt 1983; 1992). For the Johnson redder colors, $V-R_J=-0.07$ and $R_J-I_J=-0.02$ (Johnson 1966) for α Lyr. Most of photometry in different photometric band systems takes the zero point which agrees with that of the nearby colors in the standard system for A0 V stars. This also applies to the calibration of Holzman et al. (1995) for WFPC2.[2]

An exception is the definition of Thuan–Gunn *uvgr* and its CCD versions (Schneider et al. 1983, 1989). For these systems Gunn and collaborators have defined the zero point so that all magnitudes of an F subdwarf BD+17°4708 are 9.5. This definition has also been adopted in POSS II. For convenience, we give in Table 4 magnitudes of α Lyr in the Thuan–Gunn definition. Another zero point, recently more popular in the photometry work using CCD, is the AB magnitude (Oke and Gunn 1983). We assume the AB magnitude system for *ABCD* and the photometric bands for SDSS. AB magnitude is defined by $\mathrm{AB}=-2.5\log f_\nu^{\rm eff}-48.60$, where f_ν is in units of erg cm^{-2} s^{-1} Hz^{-1}. We give in Table 5 the AB magnitude of α Lyr for various photometric systems. From Tables 4 and 5 it is straightforward to calculate translation between AB or Thuan–Gunn magnitude and that defined in a conventional way, as

[2]Holzman et al. (1994) adopted $R_c=0.039$ and $I_c=0.035$ for α Lyr, instead of $Rc=0.03$ and $I_c=0.024$. Therefore, their magnitude appear fainter than the standard Cousins magnitude used in this article by R_c(Holzman)$=R_c+0.009$ mag and I(Holzman)$=I_c+0.011$ mag. For the WFPC2 photometric system we followed the definition of Holzman et al.: $F505W-V=0$; $F606W-V=0$; $F702W-R_c$ (this paper) $=0.009$; $F814-I_c$ (this paper)$=0.011$ for α Lyr.

TABLE 9
Characteristics of Photometric Bands

bandpass system	band	ref[a]	$\lambda_{\rm eff}$ (Å)	FWHM (Å)	$\lambda_{\rm eff}^{\rm Vega}$ (Å)	$f_{\lambda,\rm eff}^{\rm Vega}$ ($\times 10^{-9}$cgs/Å)	$c(\nu_{\rm eff}^{\rm Vega})^{-1}$ (Å)	$f_{\nu,\rm eff}^{\rm Vega}$ ($\times 10^{-20}$cgs/Hz)
Johnson-Morgan	U_3	Buser 78	3652	526	3709	4.28	3617	1.89
	B_2	AS69	4448	1008	4393	6.19	4363	4.02
	V	AS69	5505	827	5439	3.60	5437	3.59
Cousins	$R_{\rm C}$	Bessell 90	6588	1568	6410	2.15	6415	3.02
	$I_{\rm C}$	Bessell 90	8060	1542	7977	1.11	7980	2.38
Johnson	$R_{\rm J}$		6930	2096	6688	1.87	6693	2.89
	$I_{\rm J}$		8785	1706	8571	0.912	8545	2.28
Sandage-Smith	u		3647	595	3710	4.30	3610	1.89
	b		4466	1028	4407	6.10	4369	3.97
	v		5423	823	5368	3.75	5365	3.64
	r		6712	969	6628	1.96	6629	2.90
Strömgren	u	Olson74	3465	363	3496	3.24	3452	1.31
	v	Matsu69	4109	197	4119	7.21	4103	4.12
	b	Olson74	4668	176	4666	5.68	4663	4.15
	y	Olson74	5459	244	5455	3.62	5453	3.60
Kron	$U_{\rm K}$	Koo 85	3656	556	3737	4.32	3617	1.93
	$J_{\rm K}$		4625	1550	4537	5.54	4467	3.82
	$F_{\rm K}$		6168	1330	5978	2.64	5982	3.25
	$N_{\rm K}$		7953	1786	7838	1.17	7842	2.44
Couch-Newell	$B_{\rm J}$		4604	1490	4515	5.73	4474	3.95
	$R_{\rm F}$		6694	517	6679	1.92	6677	2.86
Thuan-Gunn	u		3536	412	3542	3.33	3519	1.38
	v		3992	469	4013	6.62	3967	3.50
	g		4927	709	4888	4.84	4885	3.89
	r		6538	893	6496	2.09	6498	2.96
Schneider et al.	g_4		5147	913	5083	4.34	5075	3.78
(4-shooter)	r_4		6659	1028	6600	1.99	6599	2.92
	i_4		8056	1604	7942	1.13	7941	2.41
	z_4		9141	1472	9071	0.797	9045	2.20
Schneider et al.	g		5238	882	5166	4.14	5160	3.74
(Pfuei)	r		6677	916	6602	1.98	6603	2.91
	i		7973	1353	7876	1.16	7876	2.43
	z		9133	984	9054	0.798	9029	2.19
Schneider et al.	A		6401	534	6384	2.19	6388	2.99
(narrow bands)	B		6904	450	6899	1.77	6895	2.81
	C		7526	608	7508	1.36	7509	2.56
	D		8087	515	8077	1.08	8075	2.35
Tyson (CCD)	$B_{\rm J}$		4614	1215	4562	5.46	4477	3.80
	R		6585	1373	6503	2.08	6504	2.97
	I		8668	1725	8532	0.928	8508	2.28
WFPC2	F555W		5536	1480	5387	3.62	5381	3.60
	F606W		6102	2050	5901	2.73	5900	3.28
	F702W		6979	1957	6826	1.77	6829	2.82
	F814W		8092	1653	7906	1.14	7923	2.43
POSS II	$g_{\rm POSS}$		5154	942	5121	4.25	5113	3.74
	$r_{\rm POSS}$		6696	1050	6632	1.96	6632	2.90
	$i_{\rm POSS}$		7837	1469	7756	1.21	7761	2.46
SDSS	u'		3585	556	3594	3.67	3530	1.54
	g'		4858	1297	4765	5.11	4748	3.93
	r'		6290	1358	6205	2.40	6210	3.12
	i'		7706	1547	7617	1.28	7623	2.51
	z'		9222	1530	9123	0.783	9098	2.19

Note — *a*) References are given whenever the response functions are taken from those which are different from the original ones. AS69 stands for Azusienis & Straizys 1969, and Matsu69 for Matsushima 1969.

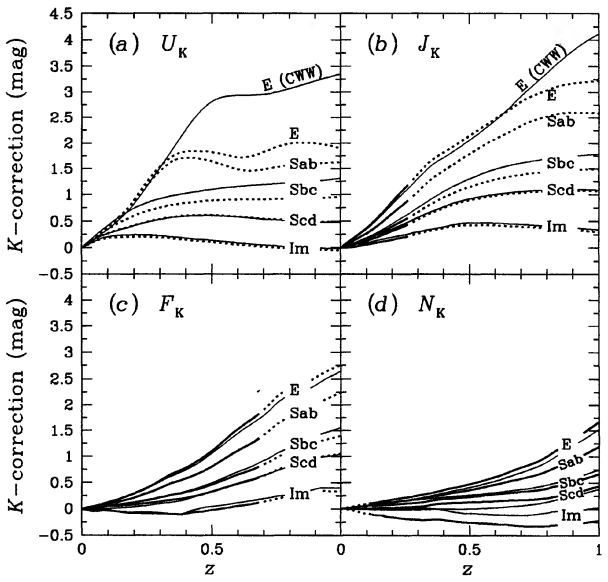

FIG. 17—K corrections for the $U_K J_K F_K N_K$ photometric system. The meaning of curves is the same as that in Fig. 10.

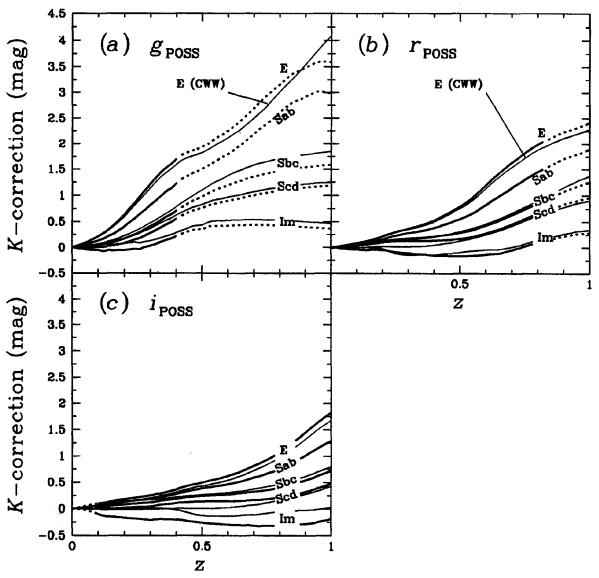

FIG. 19—K corrections for the POSS II photometric system. The meaning of curves is the same as that in Fig. 10.

$$m_{AB}=(m-c_i)+m_{AB}(\alpha\ \mathrm{Lyr}),$$

$$m_{TG}=(m-c_i)+m_{TG}(\alpha\ \mathrm{Lyr}),$$

where c_i is a small band(i)- dependent constant representing the magnitude of α Lyr in the conventional system (see Eqs.(2)-(8)). We remark that with the H85 flux zero point, the AB magnitude of α Lyr at 5480 Å is 0.012 mag, rather than 0.03 mag as it is with the Oke–Gunn zero point (Fukugita et al. 1995).

The numbers in Table 3 across the different photometric band system show that the color difference between the neighboring color bands, e.g., B and J_K or B_J, R_C and R_J, etc., is generally $\approx$0.15 mag for typical galaxies (at $z=0$); $\langle J_K-B\rangle\simeq-0.15$, $\langle B_J-B\rangle\simeq-0.12$ and $\langle J_{Ty}-B\rangle\simeq-0.13$. J_K, B_J and J_{Ty} are practically the same, allowing for errors of 0.03 mag.

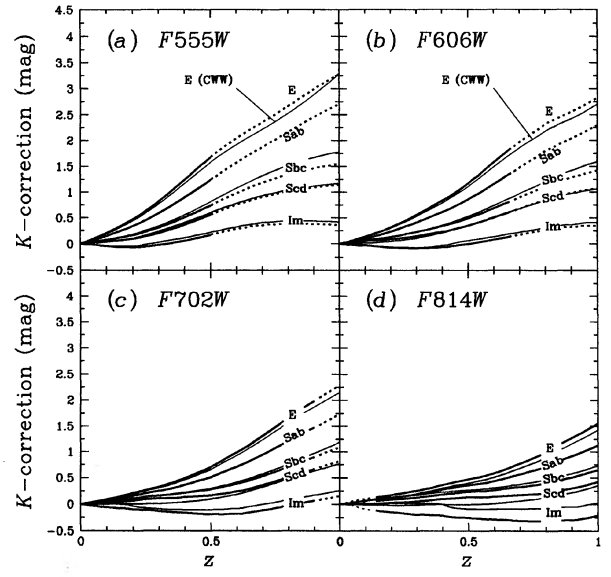

FIG. 18—K corrections for the WFPC2 photometric system. The meaning of curves is the same as that in Fig 10

Similar tables (somewhat reduced) are also given for galaxies when they are brought to $z=0.2$ (Table 6), $z=0.5$ (Table 7) and $z=0.8$ (Table 8). These tables give us transformation laws for brightness of faint galaxies observed in non-standard photometric bands into that in the standard system, either with conventional magnitudes or with AB magnitude. An interesting observation in Tables 6–8 is that the colors in neighboring bands change significantly with redshift. For instance, the color difference J_K-B for Sab galaxies, which are -0.14 at $z=0$ decreases to -0.31 at $z=0.2$, and -0.35 at $z=0.5$ (the variation is slightly less in B_J-B). This variation is particularly large, since the 4000 Å discontinuity moves to the $B-J_K$ region at $z=0.2$. For clarity, we depicted in Fig. 12(a) the difference of the K-corrections between J_K and B bands (reddening corrections are made for this figure: so the values are slightly different from those in Tables 6–8). The difference is indeed as large as 0.4 at $z\simeq0.15$ and probably more at $z\simeq0.6$. On the other hand, the transformation from J_K to B is usually taken into account merely by a constant shift of magnitude in most number count analyses. This means that the J_K count, if presented in B magnitude or compared with a calculation made for B magnitude, shows extra "brightening" by 0.2 mag from $z=0$ to $z=0.2$. This is a non-negligible effect when compared with recently achieved accuracy of the number count. A similar effect is seen with F_K and R_C bands, but at higher z, as expected from the difference of the two K corrections shown in Fig. 12(b). The offsets of U_K vs. U and N vs. I are small and stay almost at constant. Similar offsets among a few photometric systems are given in Figs. 13–16. Figure 13 shows 4-shooter versus the standard: g_4-V and r_4-R_c. i_4-I_c stays at 0.73–0.75 for the entire z range, and is omitted. The WFPC2 color versus the standard color is given in

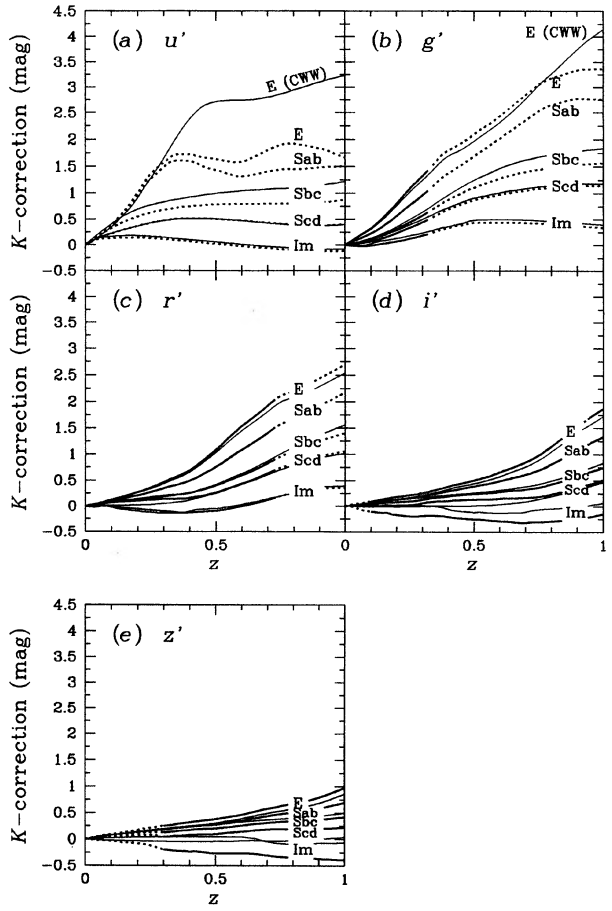

FIG. 20—K corrections for the SDSS photometric system. The meaning of curves is the same as that in Fig. 10.

Fig. 14. $F814W-I_c$ is not shown, since the curves show only a modest increase: from 0.05 at $z=0$ to 0.1 at $z=1$ for all morphological types. Figure 15 refers to the POSS II system. Figures for $r_{\rm POSS}-R_c$ (which stays at 0.65–0.8) and $i_{\rm POSS}-I_c$ (0.75 at $z=0$ increases to 0.95 (E) or 0.8 (Im) at $z=1$) are omitted. Figure 16 shows the SDSS system versus the standard colors. K corrections are also presented in Appendix B for a few photometric systems used in modern galaxy surveys.

We thank Andy Connolly, Harry Ferguson, and Don Schneider for providing us some of tables of the color response function and Y. Takeda for generating a numerical table of the CK94 SED for α Lyr. Useful discussions with Jim Gunn about the definition of the response function are gratefully acknowledged. We also thank George Djorgovsky and Edwin Turner for valuable comments improving the manuscript. This work is supported in part by Grant-in-Aid of the Ministry of Education of Japan (05101002) and Japan-US Science Programme by JSPS. K. S. is supported in part by NSF grant AST94-19400. M. F. also wishes to acknowledge generous support from the Fuji Xerox Corporation.

APPENDIX A: CHARACTERISTICS OF VARIOUS FILTERS

In Table 9 we present a compilation of characteristics of frequently used photometric bands. We take

$$\lambda_{\rm eff}=\frac{\int d\lambda\lambda R(\lambda)}{\int d\lambda R(\lambda)}, \tag{A1}$$

$$f_\lambda^{\rm eff}(\alpha\ {\rm Lyr})=\frac{\int d\lambda f_\lambda(\alpha\ {\rm Lyr})R(\lambda)}{\int d\lambda R(\lambda)}, \tag{A2}$$

$$\lambda_{\rm eff}(\alpha\ {\rm Lyr})=\frac{\int d\lambda\lambda f_\lambda(\alpha\ {\rm Lyr})R(\lambda)}{\int d\lambda f_\lambda(\alpha\ {\rm Lyr})R(\lambda)}, \tag{A3}$$

in agreement with the conventional definition. The flux of (A2) is given for the actual flux of α Lyr, rather than at zero magnitude. Hence, the flux for zero magnitude has some offset corresponding to the definition of the zero magnitude. The denominator of (A2) is close to the FWHM if the peak of the response function is normalized to unity: the difference is usually of the order of <5% except for the case of Kron J_K and N_K, the response functions of which are double peaked. For the Johnson–Morgan system, the values given in Table 9 show a very good agreement with those given in Buser (1978), where available in the latter literature. Where we adopt the definition (9), the effective lambda is defined with the flux $f_\nu\sim\nu^{-2}$, consistent with $f_\lambda=$const. in (A1).

We also give quantities similar to (A2) and (A3), but defined in terms of ν:

$$f_\nu^{\rm eff}(\alpha\ {\rm Lyr})=\frac{\int d\nu f_\nu(\alpha\ {\rm Lyr})R(\nu)}{\int d\nu R(\nu)}, \tag{A4}$$

$$\nu_{\rm eff}(\alpha\ {\rm Lyr})=\frac{\int d\nu\nu f_\nu(\alpha\ {\rm Lyr})R(\nu)}{\int d\nu f_\nu(\alpha{\rm Lyr})R(\nu)} \tag{A5}$$

where $f_\nu=\lambda^2 f_\lambda/c$ and $R_\nu=R_\lambda$.

APPENDIX B: K CORRECTIONS FOR SELECTED FILTERS

In this appendix we present K corrections for the Kron system, WFPC 2, POSS II, and SDSS photometric systems (Figs. 17–20). The Galactic absorption is corrected. The meaning of figures is the same as that for Fig. 10.

REFERENCES

Arp, H. 1961, ApJ, 133, 874
Azusienis, A. and Straizys, V. 1969, AZ, 13, 316
Bessell, M. S. 1976, PASP, 88, 557
Bessell, M. S. 1983, PASP, 95, 486
Bessell, M. S. 1990, PASP, 102, 1181
Bertola, F., Capaccioli, M., and Oke, J. B. 1982, ApJ, 254, 494
Burrows, C. J., Clampin, M., Griffiths, R. E., Krist, J., and MacKenty, J. W. 1994, Hubble Space Telescope, Wide Field and Planetary Camera 2, Instrument Handbook, version 2.0 (Baltimore, Space Telescope Science Institute)
Buser, R. 1978, A&A, 62, 411
Buser, R., and Kurucz, R. L. 1978, A&A, 70, 555
Castelli, F., and Kurucz, R. L. 1994, A&A, 281, 817 (CK94)

Code, A. D. 1960, Stars and Stellar Systems, Vol. 6: Stellar Atmospheres, ed. J. L. Greenstein (Chicago, University of Chicago Press), p. 50
Coleman, C. D., Wu, C.-C., and Weedman, D. W. 1980, ApJS, 43, 393
Couch, W. J., and Newell, E. B. 1980, PASP, 92, 746
Cousins, A. W. J. 1978, MNASSA, 37, 8
de Vaucouleurs, G., de Vaucouleurs, A., Corwin, H. G., Buta, R. J. Paturel, G., and Fouqué 1991, Third Reference Catalogue of Bright Galaxies (New York, Springer) (RC3)
Frei, Z., and Gunn, J. E. 1994, AJ, 108, 1476
Fukugita, M., Ichikawa, T., Gunn, J. E., Doi, M., Shimasaku, K., and Schneider, D. P. 1995, preprint
Gunn, J. E., and Stryker 1982, ApJS, 52, 121
Hayes, D. S. 1975, in Multicolor Photometry and the Theoretical HR Diagram, ed. A. G. D. Philip and D. S. Hayes, Dudley Observatory Report, No. 9, p.309
Hayes, D. S. 1985, in Calibration of Fundamental Stellar Quantities, IAU Symposium 111, ed. D. S. Hayes et al. (Dordrecht, Reidel) p.225 (H85)
Hayes, D. S., and Latham, D. W. 1975, ApJ, 197, 593
Holzman, J. A., Burrows, C. J., Casertano, S., Hester, J. J., Trauger, J. T., Watson, A. M., and Worthey, G. 1995, preprint
Jacoby, G. H., Hunter, D. A., and Christian, C. A. 1984, ApJS, 56, 257
Johnson, H. L. 1965, ApJ, 141, 923
Johnson, H. L., and Morgan, W. W. 1953, ApJ, 117, 313
Kennicutt, R. C. 1992, ApJS, 79, 255 (K92)
Koo, D. C. 1985, AJ, 90, 418
Kron, R. G. 1980, ApJS, 43, 305
Kurucz, R. L. 1979, ApJS, 40, 1
Landolt, A. U. 1983, AJ, 88, 439
Landolt, A. U. 1992, AJ, 104, 340
Matthews, T. A., and Sandage, A. 1963, ApJ, 138, 30
Matsushima, S. 1969, ApJ, 158, 1137
Oke, J. B., Bertola, F., and Capaccioli, M. 1981, ApJ, 243, 453
Oke, J. B., and Gunn, J. E. 1983, ApJ, 266, 713
Oke, J. B., and Schild, R. E. 1970, ApJ, 161, 1015
Olson, E. C. 1974, PASP, 86, 80
Pence, W. 1976, ApJ, 203, 39
Sandage, A., and Smith, L. L. 1963, ApJ, 137, 1057
Schild, R. and Oke, J. B. 1971, ApJ, 169, 209
Schneider, D. P., Gunn, J. E., and Hoessel, J. G. 1983, ApJ, 264, 337
Schneider, D. P., Schmidt, M., and Gunn, J. E. 1989, AJ, 98, 1507
Schneider, D. P., Schmidt, M., and Gunn, J. E. 1991, AJ, 102, 837
Straizys, V., Sudzius, J., and Kuriliene, G. 1976, A & A 50, 413
Strömgren, B. 1963, in Basic Astronomical Data, ed. K. Å. Strand (Chicago, University of Chicago Press), Vol. III, p. 131
Taylor, R. J. 1986, ApJS, 60, 577
Thuan, T. X., and Gunn, J. E. 1976, PASP, 88, 543
Turnrose, B. E. 1976, ApJ, 210, 33
Tyson, J. A. 1988, AJ, 96, 1
Wells, D. C. 1972, PhD thesis
Whitford, A. E. 1971, ApJ, 169, 215